EUROPEAN ORGANIZATION FOR NUCLEAR RESEARCH

CERN - AB Division

IONISATION CHAMBERS FOR THE LHC BEAM LOSS DETECTION

E. Gschwendtner, R. Assmann, B. Dehning, G. Ferioli, V. Kain
CERN, 1211 Geneva 23, Switzerland

Abstract

At the Large Hadron Collider (LHC) a beam loss system will be used to prevent and protect superconducting magnets against coil quenches and coil damages. Ionisation chambers will be mounted outside the cryostat to measure the secondary shower particles caused by lost beam particles. Since the stored particle beam intensity is eight orders of magnitude larger than the lowest quench level and the losses should be detected with a relative error of two, the design and the location of the detectors have to be optimised. For that purpose a two-fold simulation was carried out. The longitudinal loss locations of the tertiary halo is investigated by tracking the halo through several magnet elements. These loss distributions are combined with simulations of the particle fluence outside the cryostat, which is induced by lost protons at the vacuum pipe. The base-line ionisation chamber has been tested at the PS Booster in order to determine the detector response at the high end of the dynamic range.

IONISATION CHAMBERS FOR THE LHC BEAM LOSS DETECTION

E. Gschwendtner, R. Assmann, B. Dehning, G. Ferioli, V. Kain
CERN, Geneva, Switzerland

Abstract

At the Large Hadron Collider (LHC) a beam loss system will be used to prevent and protect super-conducting magnets against coil quenches and coil damages. Ionisation chambers will be mounted outside the cryostat to measure the secondary shower particles caused by lost beam particles.

Since the stored particle beam intensity is eight orders of magnitude larger than the lowest quench level and the losses should be detected with a relative error of two, the design and the location of the detectors have to be optimised. For that purpose a two-fold simulation was carried out: The longitudinal loss locations of the tertiary halo is investigated by tracking the halo through several magnet elements. These loss distributions are combined with simulations of the particle fluence outside the cryostat, which is induced by lost protons at the vacuum pipe.

The base-line ionisation chamber has been tested at the PS Booster in order to determine the detector response at the high end of the dynamic range.

INTRODUCTION

The magnet coil quench and damage levels are time and energy dependent. This results in a large range of loss rate variations requiring observations of ionisation chamber currents between 10^{-12} and 10^{-3} A [1]. The required time resolution for the arc monitors is 2.5 ms and for all other detectors it is 89µs (i.e. 1 LHC turn).

These requirements show already that the demands on the design of a reliable beam loss detection system are extremely high. Here are three different design aspects of the loss system are investigated:

- The longitudinal beam loss distribution of the tertiary halo along the magnets. It is emitted by the secondary collimators and will be lost at aperture limits.
- Calculations of the particle fluences outside the cryostat, which is induced by lost protons. This defines the most suitable positions, the needed number and the impact on the dynamic range of the detectors.
- The signal response of the ionisation chamber in a high rate environment similar to the LHC.

First results are shown.

TERTIARY HALO LOSS DISTRIBUTION STUDIES FOR 450 GEV

The longitudinal beam loss distribution was obtained by tracking particles populating the tertiary halo at 450GeV through parts of the LHC. The tertiary halo particles stem from the collimation insertion IR7 escaping

the secondary collimators. The halo particles were tracked with SIXTRACK and the scattering routine K2. The left plot in Fig. 1 shows the (X,Y)-distribution of the halo after the collimators. MAD-X in the 'one-pass' mode was applied to track the particles from the collimation insertion IR7 to the chain of the LHC magnet elements we investigate. Finally the linear tracking program SLICETRACK was used to slice the elements and calculate the longitudinal beam loss distribution.
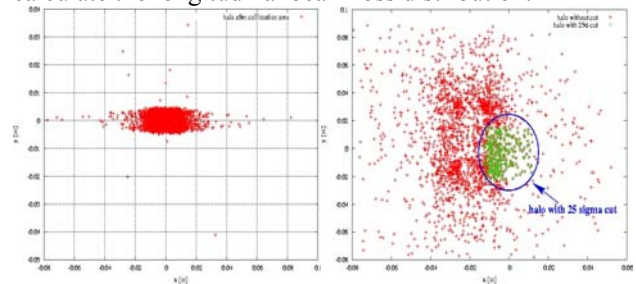

Figure 1: Left: Tertiary halo distribution after the collimation section IR7. Right: Halo tracked with MAD-X to the dispersion suppressor in IR1. Particles with amplitudes larger than 25σ are cut.

The MAD-X tracking was based on the sequence V6.4.aperture containing information on apertures in the LHC. So particles exceeding theses apertures get already lost during the transfer from the collimation section to the sliced chain of elements (e.g. tracking with MAD-X until IP5 results in the loss of all halo particles). But for the time being the LHC sequence does not contain all apertures and the particles can still reach unrealistic amplitudes in the tracking process. Thus we were forced to apply a cut in particle amplitudes before tracking through the sliced elements. Out of a geometrical argument we discarded particles with amplitudes exceeding 25σ that is still quite large (see right plot in Fig. 1).
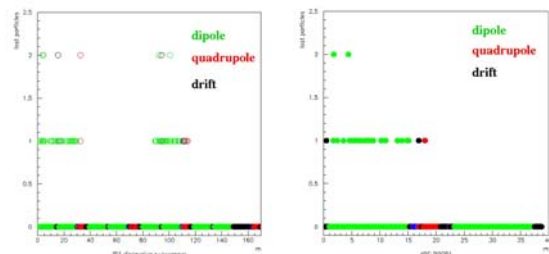

Figure 2: Loss distributions along the dispersion suppressor (left) and an arc short section (right) right of IP1. No beam excursions and misalignments are introduced.

We have investigated two cases: the loss distribution along the dispersion suppressor and along an arc short section, both right of IP1 for LHC beam1. SLICETRACK

can be used with quadrupole, dipole magnets and drifts. Different beam pipes can be simulated and several kinds of misalignment can be taken into account. It tracks the particles through these elements and compares the amplitudes with the aperture restriction after every slice of the element. No scattering is included. Aperture restrictions are treated as black absorbers.

Fig. 2 shows the loss distributions for the dispersion suppressor and the arc short section when no misalignment has been applied. Since most of the particles are off-momentum, we see that the losses happen along the bending magnets.
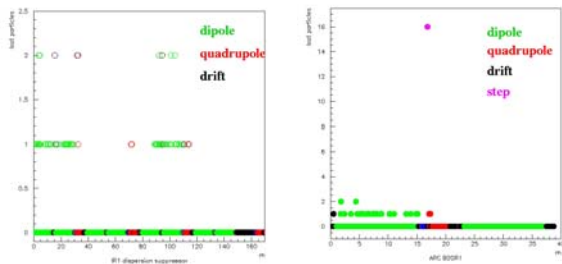

Figure 3: Left: loss distribution in the dispersion suppressor with a 4mm global beam orbit shift. Right: Losses along the arc short section when a misalignment error of 2mm in Y has been introduced.

The left plot in Fig. 3 shows the loss distribution in the dispersion suppressor when a 4mm global orbit shift has been introduced. More losses happen now in the quadrupoles. In the right plot we see that many particles in the arc short section are lost at the point where a step of 2mm in Y has been brought in.

Since the tertiary halo consists of mainly off-momentum particles, the halo is basically lost at the bending magnets and at mechanically aperture limitations. It can be assumed that the primary and secondary halo losses occur mainly at positions where the beta-functions are highest (quadrupole magnets).

EXPECTED DETECTOR SIGNALS AND POSITIONS

At the positions, where most of the beam losses occur, simulations of the particle fluences outside the cryostat and induced by lost protons at the aperture have been performed with the Monte Carlo Code Geant 3.21.
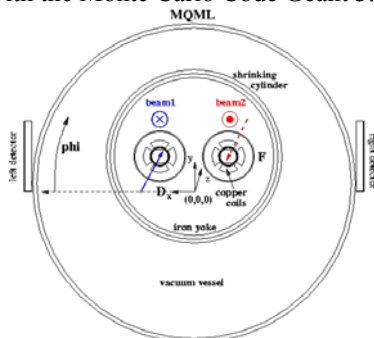

Figure 4: Cross-section of the MQML quadrupole in Q10.

The geometry used in these simulations corresponds to the dispersion suppressor layout. The arrangement consists of four quadrupole elements (Q8-Q11) separated by two dipoles (MBA, MBB), respectively. We assume that lost beam particles hit the beam screen under an angle of typically 0.25mrad in the horizontal (vertical) plane when the magnet is focusing (defocusing) in X. The simulated shower particles produced by lost protons are counted in two detector-elements placed left and right outside the cryostat (see Fig. 4).

We have already shown in Ref. [2] that the shower maximum is about 1m after the beam loss location. The shower width is 0.5m. For one proton with 7TeV lost in the middle of the magnets we observe $1 \cdot 10^{-2}$ charged particles/p/cm^2 in the detector. Several following (smaller) shower peaks are due to the gap between the magnets.
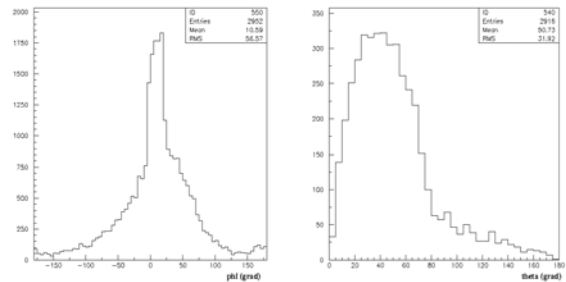

Figure 5: Left: Phi-distribution of particles escaping the cryostat. Right: Theta-distribution of particles escaping the cryostat.

The left plot in Fig. 5 shows the phi-distribution of the particles around the cryostat. Most of the particles escape the vacuum vessel in the plane of the beam-tube which corresponds to an angle of phi = 9-12 degree. In the right plot the theta-distribution (angle between the particle momentum and the X-axis) of the particles are shown. The average is theta = 50 degree.

In addition the energy deposition in the detector elements (filled with air) is calculated. With a beam energy of 7TeV (450GeV) the energy deposition is ~4.3keV/cm (3.8 keV/cm).

A summary of the signal rates for the different energies and loss distributions is given in Ref. [2] and [3].

TESTS OF THE IONISATION CHAMBER IN THE PS BOOSTER

The ionisation chamber has been tested in the PS Booster at different beam intensities in terms of signal shape, linearity response and electron and ion induced signal.

A photo of the detector is shown in Fig. 6. The baseline layout is a N$_2$ filled cylinder with a surface of 80cm^2, a radius of 4.75cm, consisting of 30 gaps separated by 1mm thick Aluminium discs and a gap-width of 0.55cm. A typical bias voltage is 1500V.

The detector was placed in the beam-line in front of the beam-dump. The energy of the protons in the beam and passing through the detector was E_{kin}=1.4GeV, the duration of a spill was 50ns. The beam intensity varied between $5 \cdot 10^8$ to $1 \cdot 10^{10}$ protons/spill. The size of the beam at the detector has been estimated to be $\sigma_{horiz.}$ = 3.5mm and $\sigma_{vert.}$= 3.5mm and 1.7mm.

Figure 6: Photo of an ionisation chamber.

The number of electron/ion pairs N created along the detector per 1 proton can be calculated with

$N=cluster/cm \cdot electron/cluster \cdot gap\text{-}width \cdot nr\text{-}of\text{-}gap.$

With *cluster/cm*=23, *electrons/cluster*=1.89, *gap-width*=0.55cm and *number-of-gaps*=30 we get *N*=717electron/ion pairs per 1 proton. From the ionisation chamber signal we can now recalculate the number of protons *MP* that passed through the detector with

$MP=\int V(t)dt / (N \cdot R \cdot e)$

with *e,* the elementary charge, *N*=717el/ion pairs per 1 proton, *R*=50Ω and $\int V(t)dt,$ the measured voltage signal integrated over 300μs (89μs) that is induced by both the electrons and the ions (see Fig. 7).
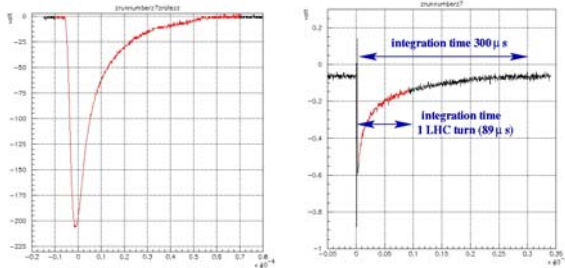

Figure 7: Electron (left plot) and ion (right plot) induced signal in the ionisation chamber from a PS Booster intensity of $9 \cdot 10^9$ protons/spill.

The left plot in Fig. 8 compares the measured proton intensity integrated over 300μs and 89μs, respectively, versus the PS Booster intensity. We see at higher intensities ($1 \cdot 10^{10}$ protons/spill) a non-linear response of the ionisation chamber. However, the right plot of Fig. 8 shows that the ratio of the measured intensity for 89μs and 300μs integration times does not depend on the beam intensity.
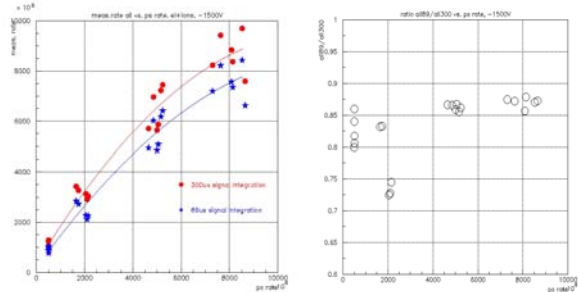

Figure 8: Left: Measured proton intensity vs. PS Booster intensity. Right: Ratio of measured intensity for 89μs and 300μs integration times vs. PS Booster intensity.

SUMMARY

The loss distribution calculations of the tertiary halo show that losses concentrate around the bending magnets due to the non nominal momentum of the majority of protons and also around positions where mechanical limitations of the aperture can be assumed.

The shower simulations show that the phi-distribution of the shower particles is independent of the loss location both in the beam tube and along the magnets.

Tests of the ionisation chamber in the PS Booster show that the electrons and ions are collected in less than 300μs. At high intensities ($1 \cdot 10^{10}$ protons) a non-linear response of the ionisation chamber is observed. The error does not depend on the beam intensity when integrating the signal every LHC turn (89μs).

REFERENCES

[1] B. Dehning, CERN-AB-2003-008 ADM, Proceedings of the Workshop on LHC Performance, Chamonix XII, France (2003).

[2] E. Gschwendtner et al., 8th European Particle Accelerator Conference, La Vilette, Paris, France, (2002).

[3] A. Arauzo-Garcia et al., CERN-SL-2001-027-BI, CERN, (2001).